

---

# EXPECTATION MAXIMIZATION PSEUDO LABELLING FOR SEGMENTATION WITH LIMITED ANNOTATIONS

---

**Mou-Cheng Xu**  
UCL, UK  
xumoucheng28@gmail.com

**Yukun Zhou**  
UCL, UK

**Chen Jin**  
AstraZeneca, UK

**Marius de Groot**  
GSK, UK

**Daniel C. Alexander**  
UCL, UK

**Neil P. Oxtoby**  
UCL, UK

**Yipeng Hu**  
UCL, UK

**Joseph Jacob**  
UCL, UK

## ABSTRACT

We study pseudo labelling and its generalisation for semi-supervised segmentation of medical images. Pseudo labelling has achieved great empirical successes in semi-supervised learning, by utilising raw inferences on unlabelled data as pseudo labels for self-training. In our paper, we build a connection between pseudo labelling and the Expectation Maximization algorithm which partially explains its empirical successes. We thereby realise that the original pseudo labelling is an empirical estimation of its underlying full formulation. Following this insight, we demonstrate the full generalisation of pseudo labels under Bayes' principle, called Bayesian Pseudo Labels. We then provide a variational approach to learn to approximate Bayesian Pseudo Labels, by learning a threshold to select good quality pseudo labels. In the rest of the paper, we demonstrate the applications of Pseudo Labelling and its generalisation Bayesian Pseudo Labelling in semi-supervised segmentation of medical images on: 1) 3D binary segmentation of lung vessels from CT volumes; 2) 2D multi class segmentation of brain tumours from MRI volumes; 3) 3D binary segmentation of brain tumours from MRI volumes. We also show that pseudo labels can enhance the robustness of the learnt representations. The code is released in the following GitHub repository: <https://github.com/moucheng2017/EMSSL>.

**Keywords** Pseudo Labels · Expectation-Maximization · Semi-Supervised Learning · Robustness · Variational Inference

## 1 Introduction

### 1.1 Label scarcity: one major bottleneck of deep learning in medical imaging

Medical image segmentation is to accurately label pixels of interest in medical images, as a foundational step towards a broad range of downstream tasks such as computer-aided diagnosis, real-time surgical navigation, drug discovery and so on. Recent years have seen rises of deep learning enabled medical image segmentation methods for more accurate and faster segmentation results. However, there is no free lunch. According to the scaling laws [1], given fixed computational resources and model sizes, the performances of deep learning models depend on the amount of paired data and labels. Unfortunately, it is notoriously difficult to acquire a large amount of annotations for segmentation of medical images because of the high costs of money and time. Unlike natural images which are normally 2D, medical images are usually volumetric with high resolution, making the pixel-level annotation process exponentially more labour intensive than standard image segmentation tasks in computer vision. In addition, the annotation process of medical images require highly skilled medical experts which are extra costly.

To address the unavoidable label scarcity issue in medical image segmentation, semi-supervised learning has been introduced to jointly train on both labelled and unlabelled data to bootstrap the model performance. The unlabelled images normally have a much larger quantity than the labelled ones, but they are normally ignored in supervised learning. Semi-supervised learning is attractive because it improves the model by using the existing resource of unlabelled images, avoiding investments in label acquisitions. Apart from semi-supervised learning for addressing label scarcity,

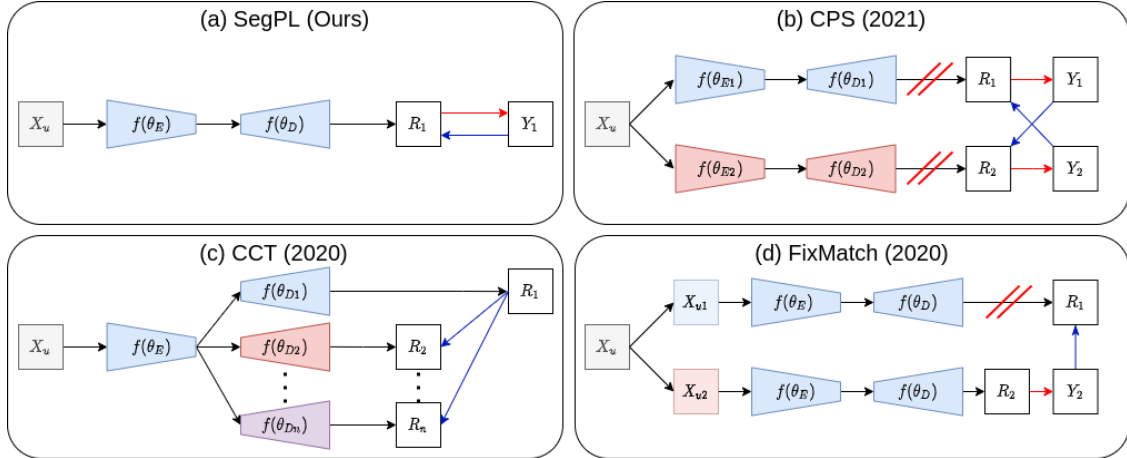


Figure 1: Comparison between pseudo labelling approach (SegPL) and the other approaches. Pseudo labelling approaches enjoy simplicity in implementation including corresponding benefits such as scalability and robustness.

other approaches have also been invented such as outsourcing data labelling [2] combined with federated learning. However, semi-supervised learning still remains attractive as it has a good trade-off balance between the cost and the improvements of the models. The current paper focuses on semi-supervised learning.

## 1.2 Brief review of semi-supervised learning

Most of the semi-supervised learning methods aim at minimising the entropy of predictions of unlabelled data in order to make “firm” predictions. Entropy minimisation has a long history in representation learning. One of the earliest form of entropy minimisation was derived from the mutual information between the input and output in unsupervised learning [3]. Entropy regularisation gained tremendous popularity in semi-supervised image classification after the authors in [4] proposed to minimise the entropy on unlabelled data as a strong regularisation to drive the model to learn a good decision boundary. Since then, entropy minimisation has been evolving from its original explicit form to varying implicit forms.

Among different implicit forms of entropy minimisation, consistency regularisation is the most common one and it is behind most of the recent state-of-the-art methods in semi-supervised classification and segmentation [5]–[9]. There are mainly two types of consistency regularisation, one is soft consistency regularisation which applies distance based loss directly on the raw outputs or the probabilities of predictions, the other type is hard consistency regularisation which transforms raw outputs to pseudo label to supervise the raw outputs or the probabilities of predictions. Both types of the consistency regularisation [5], [6], [9]–[11] enforce the deep learning models to make predictions which are invariant to the perturbations at the input level or the feature level [8], [9], [12], [13]. For methods with consistency regularisation on input level, a lot of them are derived from a classic method called Mean-Teacher [10]. The mean-teacher model has two models, the weight of the student model is the exponential moving averaging weights of the teacher model. The teacher model intakes a normal input while the student model intakes the same input but added with Gaussian noise, a mean square error is used for soft consistency regularisation between the outputs of the teacher and the student model. Another more advanced teacher-student model called FixMatch achieved state-of-the-art performance in semi-supervised classification [5]. In FixMatch [5], the model intakes two forward passes, one pass with weakly augmented (e.g. flipping) input and the other one pass with strongly augmented (e.g. shearing, random intensity) input. Then the output of the weakly augmented input will be used to generate a pseudo label as the ground truth for training the output of the strongly augmented input, the workflow of FixMatch is illustrated in (d) in Fig.1. Although FixMatch and its variants have achieved great successes in image classification, it was noticed that it was not straightforward to directly apply FixMatch-style methods in image segmentation, because the cluster assumption does not hold at pixel-level in dense prediction tasks [8]. To adopt consistency regularisation in segmentation, the authors in [12] have discovered that it is possible to apply perturbations on the features for instead of inputs before the consistency regularisation is applied. In [12], the authors directly apply augmentation techniques on the features of different decoders before the consistency regularisation (see (c) in Fig.1) for semi-supervised image segmentation. Apart from adding directly perturbations on the features directly, it is also feasible to add perturbations on the features through architectural modifications. For example, one can train two identical models but with different initialisation and apply consistency regularisation with

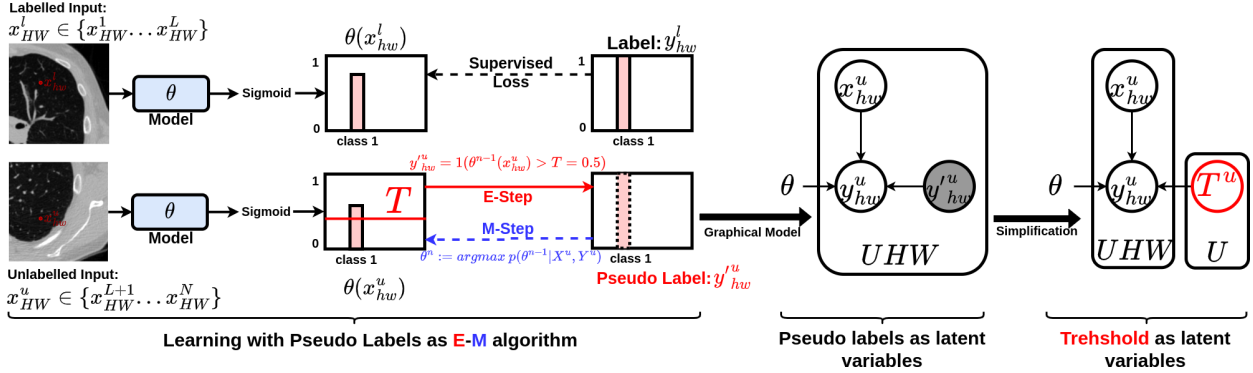


Figure 2: Pseudo-labelling process for binary segmentation. Pseudo-label  $y'_n$  is generated using unlabelled data  $x_u$  and model with parameters from last iteration  $\theta$ . Therefore, pseudo-labelling can be seen as the E-step in Expectation-Maximization. The M-step updates  $\theta$  using  $y'_n, y$  and data  $X$ . In our 1st implementation, namely SegPL, the threshold  $T$  is fixed for selecting the pseudo labels, which is the original pseudo labelling, as an empirical approximation of its true generalisation. In our 2nd implementation, namely SegPL-VI, the threshold  $T$  is dynamic and learnt via variational inference, which is an learnt approximation of its true generalisation.

pseudo labels on the two outputs [13] (Fig1 (b)) also for semi-supervised image segmentation. The aforementioned methods have also been tested and compared against our method in later section.6.

### 1.3 Motivations and contributions

It has come to our attention that most of the existing pseudo labelling papers are purely empirical without investigating the reason behind its empirical successes. Therefore we decided to revisit pseudo labelling and we noticed that pseudo labelling has a deep connection with the classical machine learning approach Expectation Maximization. Our second motivation is inspired by a recent paper in semi-supervised image classification, showing that it is entirely possible to achieve competitive results with smartly selected good quality pseudo labels [14]. In this paper, we build up our insight of pseudo labelling on the Expectation Maximization algorithm, we as well provide empirical investigations of pseudo labelling in semi-supervised medical image segmentation and its robustness. A shorter version of this paper has been published at MICCAI 2022 [15]. We summarize our contributions in the following bullet points.

- We interpret pseudo labelling as Expectation Maximization (EM) algorithm. As EM algorithm is guaranteed to converge to local minimum. We therefore partially explain the empirical success of pseudo labelling.
- We provide a learning method to find the generalised pseudo labels using variational inference.
- We investigate the use of pseudo labelling in semi-supervised medical image segmentation and its characteristics such as robustness.

## 2 Related works

### 2.1 Pseudo Labelling

The original pseudo labelling [16] was proposed for semi-supervised multi-class image classification. In the original pseudo labelling, the pseudo labels are created as  $\arg \max$  outputs (same as running the inferences) on the predictions on the unlabelled data. The created pseudo labels are used to train the unlabelled data following standard supervised learning fashion. The original pseudo labelling actually creates the pseudo label online on-the-fly. It was also suggested to carefully use the pseudo labels that one should first warm-up the model with only supervised learning, then gradually ramp-up the weight of the pseudo supervision. Pseudo labelling has become popular in semi-supervised learning because it is computationally cheap but with good performance. It has been shown that semi-supervised learning can surpass its supervised learning counterpart [17] on ImageNet classification by using pseudo labelling on an internet-level unlabelled data. Another recent work breaks the trend of growing complexity of consistency regularisation methods and achieved competitive results with only pseudo labels[14] in semi-supervised image classification. In image segmentation, a pseudo labelling approach has also achieved impressive results [18] whereas the pseudo labels are refined with self-attention mechanism. Pseudo labelling also has its own potential issue which is called confirmation

bias [19] that if wrong pseudo labels are used, noisy training will happen and the errors will be accumulated and potentially amplified. This potential issue inspired us and in later section, we will introduce a stochastic training of pseudo labels that learns to pick up pseudo labels.

## 2.2 Semi-supervised learning in medical image segmentation

Most of the existing methods for semi-supervised segmentation are stemmed from the methods in semi-supervised classification described in the previous section. For example, mean-teacher based consistency regularisation methods have been popular in semi-supervised medical image segmentation [20]–[29]. One of the earliest mean-teacher model in medical imaging was proposed by Yu [30], they improve on mean-teacher model by using uncertainty to generate a mask to apply consistency regularisation only on low-uncertainty areas. In addition to data level perturbations, feature level perturbations based consistency regularisation area also popular. For instance, Luo [31] uses different initialisation of different decoders to achieve feature perturbations. Xu [9] uses differential morphological operations to add feature perturbations in the decoders before consistency regularisation. Pseudo labelling approaches have also been previously explored in medical image segmentation. Bai [32] used conditional random field to remove the false positives of the pseudo labels. Wang [33] uses uncertainty to refine pseudo labels. Wu [34] combines pseudo labels with two headed network to form a cross pseudo supervision. Another recent work [35] uses variational auto-encoder as student model and learns from pseudo labels which generated by deterministic teacher model.

## 3 Pseudo Labelling As Expectation-Maximization

In this section, we provide a new perspective of semi-supervised learning with pseudo labels as the Expectation-Maximization (EM) algorithm. We focus on a binary segmentation case as most of medical image segmentation tasks are binary ones on differentiating the foreground area from the background area. Multi-class segmentation can be trivially extended from the binary case with multi-channel Sigmoid, by separately treating each channel as a binary output, combining with the argmax operation before the final prediction.

### 3.1 Problem formulation

Given a set of  $N$  total available training images as  $X = \{x_n \in R^{HW} : n \in (1, 2, \dots, L, L + 1, \dots, N)\}$ , where  $X_L = \{x_l \in R^{HW} : l \in (1, \dots, L)\}$  are  $L$  labelled images;  $Y_L = \{y_l \in R^{HW} : l \in (1, \dots, L)\}$  are  $L$  labels for  $X_L$ ;  $X_U = \{x_u \in R^{HW} : u \in (L + 1, \dots, N)\}$  is the rest of the  $U$  or  $(N - L)$  unlabelled images. We have a segmentation network with parameters as  $\theta$  and our final goal is to predict the labels  $p(Y|X, \theta)$  of the whole data  $X$  with respect to  $\theta$ .

### 3.2 Pseudo labels as latent variables

In order to find the optimal parameters of  $\theta$ , the common approach is maximum likelihood estimation for maximising the likelihood of  $P(X|\theta)$  with respect to  $\theta$ , which contains two parts, namely supervised learning part and unsupervised learning part. The supervised learning part is to find the following joint data density with known full information of the labels:

$$p(X_L, Y_L|\theta) \tag{1}$$

The unsupervised learning part is to find the beneath likelihood with the same parameters without full information of the data:

$$p(X_U|\theta) \tag{2}$$

Since labels are not observable for  $X_U$ , we can treat this as a missing data problem and introduce latent variables  $Y'_U$ . We therefore transform the above Eq. 2 to an estimation of the following marginal likelihood:

$$p(X_U|\theta) = \int p(X_U, Y'_U|\theta) dY'_U \tag{3}$$

We notice that the generation of pseudo-labels naturally poses a generative task. We also observe that the pseudo labels are only used as an intermediate step towards the final prediction of the labels. Thereby we propose to treat pseudo-labels as an implementation of the latent variables in the above Eq. 3. Eq. 3 also shows that it is not an easy task to train a model in semi-supervised fashion, because it is difficult to simultaneously estimate the optimal values of two different sets of variables. To address this difficult learning problem, we can decompose this problem by iteratively estimating the the latent variables  $Y'_U$  and the observed variable  $X_U$ . We now notice that this can be solved by a typical Expectation-Maximization (EM)[36] algorithm. By plugging the Jensen’s inequality, one can iteratively refine the Evidence Lower Bound of the log likelihood of the data in Eq.3

### 3.3 E-M Pseudo Labelling

We now display each component of the pseudo labelling in the sense of EM algorithm in the following paragraphs.

**E-step** At the  $n^{th}$  iteration, the E-step estimates the posterior of the latent variable with the model  $(\theta^{n-1})$  from the last iteration  $(n-1)$ . According to the cluster assumption that similar data points are supposed to have similar labels [37], the E-step runs the inference on unlabelled data and generate pseudo-labels according to its maximum predicted probability. In practice, in binary segmentation, the pseudo-labels for the foreground class 1 are picked using a fixed threshold value  $(T)$  between 0 and 1. Normally, this threshold is set up as 0.5. This binarization is actually equivalent to the plug-in principle [4], which is a common approach for estimating the posterior probability using an empirical estimation in statistics. Therefore, the pseudo-labelling itself is the E-step:

$$y_u^{hw'} = \mathbb{1}(\theta^{n-1}(x_u^{hw}) > T = 0.5) \quad (4)$$

The above Eq. 4 is pseudo-labelling at pixel-wise. Where  $h$  and  $w$  are the index for the height and the index for the width of the pixel location respectively, for each unlabelled image  $x_u$ .  $y_u^{hw'}$  is the pixel-wise pseudo label. More details of the connection between E-step and pseudo labelling is in the later section sec.3.4 on the convergence of pseudo labelling.

**M-step** At the M-step of iteration  $n$ , we will update the model parameters  $\theta^{n-1}$  using the estimated latent variables (pseudo-labels  $Y'_U$ ) from the E-step. The images  $X$  are ignored for simplicity in the following expression (e.g. differing from the MICCAI version):

$$\theta^n := \underset{\theta}{\operatorname{argmax}} p(\theta^n | \theta^{n-1}, Y'_U) \quad (5)$$

The above Eq.5 is normally solved by setting the partial derivatives of the sum of the  $p(Y'_U)$  with respect to  $\theta$  as zero, which can be calculated with modern automatic differentiation based deep learning toolbox such as Pytorch [38]. In practice, we solve Eq.5 via stochastic gradient descent. To use the stochastic gradient descent, we need to define an objective function and we use the common Dice loss ( $f_{dice}(\cdot)$ ) [39] as this is a segmentation task:

$$f_{dice}(a, b) = \frac{2 * a * b + \epsilon}{a + b + \epsilon} \quad (6)$$

**Loss function of SegPL** We weight the Eq.5 with a hyper-parameter  $\alpha$ . For the whole data set including both unlabelled and labelled data, we can extend the Eq.5 and Eq.4 to a combination between the supervised learning part  $L_L$  and the unsupervised learning part  $L_U$ :

$$\begin{aligned} \mathcal{L}_{SegPL} = & \alpha \underbrace{\frac{1}{N-L} \sum_{u=L+1}^N f_{dice}(\theta^{n-1}(x_u), \mathbb{1}(\theta^{n-1}(x_u) > T = 0.5))}_{\mathcal{L}_U} \\ & + \underbrace{\frac{1}{L} \sum_{l=1}^L f_{dice}(\theta^{n-1}(x_l), y_l)}_{\mathcal{L}_L} \end{aligned} \quad (7)$$

The above loss function 7 is the key component of our first proposed semi-supervised segmentation method, omitting pixels' locations for simplicity, which is referred as SegPL (Segmentation with Pseudo Labels) in the paper.  $\mathcal{L}_L$  works to prevent the networks falling into trivial solutions, trivial solutions happen when networks constantly predict one single class for all of the pixels.

### 3.4 On the convergence of Pseudo Labelling from the perspective of EM

In this section, we explain how semi-supervised learning with pseudo-labelling will always converges from the perspective of EM. We first define a target function as  $l(\theta)$ , in our case, it would be the log likelihood of the data  $X$ . We also need to introduce a surrogate function  $q(Y'_U)$  which is any arbitrary distribution over the latent variable  $Y'_U$ . We

follow [36] and show the lower bound of the data likelihood in the form of the Free Energy of the generative latent variable model:

$$\begin{aligned}
l(\theta) &:= \log \int p(X_U, Y'_U | \theta) dY'_U \\
&\stackrel{\text{Eq.3}}{=} \log \int q(Y'_U) \frac{p(X_U, Y'_U | \theta)}{q(Y'_U)} dY'_U \\
&\geq \int q(Y'_U) \log \frac{p(X_U, Y'_U | \theta)}{q(Y'_U)} dY'_U \\
&= \underbrace{\int q(Y'_U) \log p(X_U, Y'_U | \theta) dY'_U}_{\text{Definition of Expectation}} - \underbrace{\int q(Y'_U) \log q(Y'_U) dY'_U}_{\text{Entropy of surrogate function}} \\
&:= \underbrace{\mathcal{F}(q(Y'_U), \theta)}_{\text{Free Energy}}
\end{aligned} \tag{8}$$

We now show another decomposition of the data likelihood starting from the free energy:

$$\begin{aligned}
&\mathcal{F}(q(Y'_U), \theta) \\
&= \int q(Y'_U) \log \frac{p(X_U, Y'_U | \theta)}{q(Y'_U)} dY'_U \\
&= \int q(Y'_U) \log \frac{p(Y'_U | X_U, \theta) p(X_U | \theta)}{q(Y'_U)} dY'_U \\
&= \int q(Y'_U) \log p(X_U | \theta) dY'_U + \int q(Y'_U) \log \frac{p(Y'_U | X_U, \theta)}{q(Y'_U)} dY'_U \\
&:= \log p(X_U | \theta) - KL[q(Y'_U) || p(Y'_U | X, \theta)] \\
&= l(\theta) - KL[q(Y'_U) || p(Y'_U | X, \theta)]
\end{aligned} \tag{9}$$

The meaning of the last decomposition in the Eq.9 is that, for any fixed  $\theta$ , the free energy term has an upper bound by the log likelihood of the data  $l(\theta)$  because KL can never be negative. In order to reach that upper bound when  $\theta$  is fixed, we need to minimise  $KL[q(Y'_U) || p(Y'_U | X, \theta)]$ . The KL distance has its minimum value at zero only if  $q(Y'_U)$  is equal to  $p(Y'_U | X, \theta)$ . Therefore, for given fixed model parameters, we can reach the upper limit of the lower bound, by simply replacing the arbitrary function of latent variable as the current estimated posterior of the latent variable:

$$q(Y'_U) = p(Y'_U | X_U, \theta) \tag{10}$$

The above Eq.10 is actually the E-step and pseudo labelling in Eq.5 is doing exactly the same thing as in Eq.10.

We now explain how M-step increases the log likelihood too. We need to rewrite the log of data likelihood by combing Eq.8 and Eq.9:

$$l(\theta) = \underbrace{\mathcal{F}(q(Y'_U), \theta)}_{\text{lower bound}} + KL[q(Y'_U) || p(Y'_U | X, \theta)] \tag{11}$$

The subsequent M-step is applying supervised learning to optimise the model parameters with fixed pseudo labels which are produced from the precursory E-step. As supervised learning can be seen as maximum likelihood estimation, thereby, M-step increases the likelihood as if the latent variables were observed, resulting in rising the data likelihood's lower bound [36]. In the above Eq.11, the  $q(Y'_U)$  is fixed but estimated from the old parameters  $\theta^{n-1}$  whereas the posterior of the latent variable is now updated as  $p(Y'_U | X, \theta^n)$ , therefore they are not equal anymore and the KL term will become a positive value. Together, it is easy to tell that the M-step increases the data log likelihood by at least the increased amount of the lower bound.

Until now, it is clear to see that, how the pseudo labelling (E-step), combined with semi-supervised optimisation of model parameters (M-step) can never decrease the likelihood of the data, leading to guaranteed convergence towards local optima [40]. In summary, the entire process of increasing data log likelihood can be expressed as in Eq.12:

$$l(\theta^n) \geq \underbrace{\mathcal{F}(q(Y'_U)^n, \theta^n)}_{\text{Jensen's ineq.}} \geq \underbrace{\mathcal{F}(q(Y'_U)^n, \theta^n)}_{\text{M-step}} \geq \underbrace{\mathcal{F}(q(Y'_U)^n, \theta^{n-1})}_{\text{E-step}} = l(\theta^{n-1}) \tag{12}$$

## 4 Generalisation of Pseudo Labels via Variational Inference for Segmentation

In the last section 3, we use an empirical estimation of the posterior of the latent variables (pseudo labels) by setting the  $T$  as 0.5. The fixed empirical estimation of  $T$  could be sub-optimal especially in the early stage of training when the networks do not have good representations and the predictions are not very confident [14]. Potentially, noisy training with some “bad” pseudo labels could accumulate some errors into the learnt representations. To address this potential issue, we provide an alternative approach to learn to approximate the true posterior of the pseudo labels. This alternative approach can be seen as a generalisation of the empirical estimation approach in SegPL in section 3.

### 4.1 Confidence threshold as latent variable

In the last section 3, we directly treat pseudo labels as latent variables. However, in segmentation task, the pseudo labels are pixel-wise, making the generative task a difficult one. To address this, we now introduce a simplification of the graphical model of the pseudo-labelling in 3. The key of this simplification is to treat the threshold value  $T$  as the latent variable which is a single value for each image:

$$p(X_U|\theta) = \int p(X_U, T|\theta)dT \quad (13)$$

This simplification makes the computation of the posterior much easier. Firstly, we have a prior knowledge of the range of this single value  $T$ , that any distribution describing values between 0 and 1 can be used as a prior distribution to approximate the real distribution of  $T$ . Secondly, the approximation of a single value  $T$  is intrinsically simpler than the approximation of pixel-wise unknown labels  $Y'$ . To see why the approximation of the true posterior of  $Y'$  is very difficult one, we write down the posterior of  $T$  with Bayes' rule:

$$p(T|X_U, \theta) = \frac{p(X_U|T, \theta)p(T)}{p(X_U|\theta)} \quad (14)$$

The new E-step at iteration  $n$  with threshold as the latent variable now becomes:

$$p(T_n = i|X_U, \theta^{n-1}) = \frac{\prod_{u=L+1}^N p(x_u|\theta^{n-1}, T_n = i)p(T_n = i)}{\sum_{j \in [0,1]} \prod_{u=L+1}^N p(x_u|\theta^{n-1}, T_n = j)p(T_n = j)} \quad (15)$$

From the above Eq.15, one can tell that the empirical estimation of the threshold  $T$  is actually necessary although not optimal. Even after a major simplification of the latent variables, the posterior of the pseudo-labels is still intractable. Because there are infinite possible values between 0 and 1 in the denominator in Eq. 15.

### 4.2 Variational E-step

To address the aforementioned intractable issue in Eq. 15, we use variational inference for the approximation of  $p(T)$ . Luckily, after the above simplification of the graphical model, we actually have a clear prior of  $T$  to match, which is any distribution describing values between 0 and 1. For the implementation simplicity, we adapt an univariate Normal distribution for the prior distribution and we denote the prior distribution of  $T$  as a surrogate distribution  $q(\beta)$ . We use extra model parameters  $\phi$  to parameterize the log variance and the mean of the approximated posterior distribution of  $T$ , conditioning on the image features, see the beneath Eq. 17.  $\phi$  is implemented as a average pooling layer followed by a single 3 x 3 convolutional block including ReLU and normalisation layer, then two 1 x 1 convolutional layers for  $\mu$  and  $\text{Log}(\sigma^2)$  respectively. Alternatively, a simple fully connected layer can also be used as  $\phi$ , we found no performance differences among different choices of architectures for  $\phi$ .

$$(\mu, \text{Log}(\sigma^2)) = \phi(\theta(X_U)) \quad (16)$$

$$p(T|X_U, \theta, \phi) \approx \mathcal{N}(\mu, \sigma) \quad (17)$$

Differing from the fixed  $T$  in E-step in Eq. 4, the  $T$  in variational E-step is dynamic, we denote the stochastic threshold as  $\mathbf{T}$  for clarity. We use the standard reparameterization trick [41] to generate the threshold in each iteration:

$$\begin{aligned}\mathbf{T} &= \mu + rand * e^{0.5 * \log(\sigma^2)} \\ rand &\sim \mathcal{N}(0, 1)\end{aligned}\tag{18}$$

As demonstrated in previous Eq.11 that the data likelihood term has an Evidence Lower Bound (ELBO) which contains a conditional probability of the data given latent variable and a KL distance between the posterior and the prior of the latent variable. We therefore write down variational unsupervised learning objective as:

$$\begin{aligned}Log(P(X_U)) &\geq \\ \sum_{u=L+1}^N \mathbb{E}_{T \sim P(\mathbf{T})} [Log(P(x_u | \mathbf{T}))] &- KL(p(\mathbf{T}) || q(\beta))\end{aligned}\tag{19}$$

**Loss function of BPL** The new learning objective  $P(X, \mathbf{T}, \theta)$  over the whole data set has a supervised learning  $P(X_L, \mathbf{T}, \theta)$  which has not changed from Eq. 7, and an unsupervised learning part  $P(X_U, \mathbf{T}, \theta)$  from the above Eq. 19. The final loss function is an ELBO over the whole data set:

$$\begin{aligned}\mathcal{L}_{SegPL}^{VI} &= \underbrace{\frac{1}{L} \sum_{l=1}^L f_{dice}(\theta^{n-1}(x_l), y_l)}_{\mathcal{L}_L} + \\ \alpha \frac{1}{N-L} \sum_{u=L+1}^N f_{dice}(\theta^{n-1}(x_u), \mathbb{1}(\theta^{n-1}(x_u) > \mathbf{T})) &+ \\ \underbrace{Log(\sigma_\beta) - Log(\sigma) + \frac{\sigma^2 + (\mu - \mu_\beta)^2}{2 * (\sigma_\beta)^2} - 0.5}_{\mathcal{L}_{KL}: KL(p(\mathbf{T}) || q(\beta)), \beta \sim \mathcal{N}(\mu_\beta, \sigma_\beta)}\end{aligned}\tag{20}$$

Where  $\mathbf{T}$  can be found in Eq. 18. Different data sets might need different priors for the best empirical performances. For example, we found that  $\beta \sim \mathcal{N}(0.4, 0.1)$  works well for CARVE. For BRATS, we didn't tune the prior and simply adopted  $\beta \sim \mathcal{N}(0.5, 0.1)$ . However, according to the result of the ablation study on the prior values in Fig.??, we might suggest to the future users to start from a high value starting from 0.9.

## 5 The connection between Bayesian Pseudo Label and Variational Autoencoder

We would like to clarify that the proposed BPL is different from Variational Auto Encoder (VAE) [41]. First of all, our BPL and VAE implement the latent variables differently as shown in Fig.3. Also, VAE has a likelihood term on the data reconstruction  $p(x')$ , while BPL estimates the likelihood  $p(y')$  of the label of unlabelled data. In addition, VAE is fully unsupervised while BPL is semi-supervised.

## 6 Experimental Results

### 6.1 Data sets

**The classification of pulmonary arteries and veins (CARVE)** We use CARVE for demonstration of 3D binary segmentation of lung vessel of CT images. The CARVE dataset [42] comprises 10 fully annotated non-contrast low-dose thoracic CT scans. Each case has between 399 and 498 images, acquired at various spatial resolutions ranging from (282 x 426) to (302 x 474). We randomly select 1 case for labelled training, 2 cases for unlabelled training, 1 case for validation and the remaining 5 cases for testing. All image and label volumes were cropped to  $176 \times 176 \times 3$ . To test the influence of the number of labelled training data, we prepared four sets of labelled training volumes

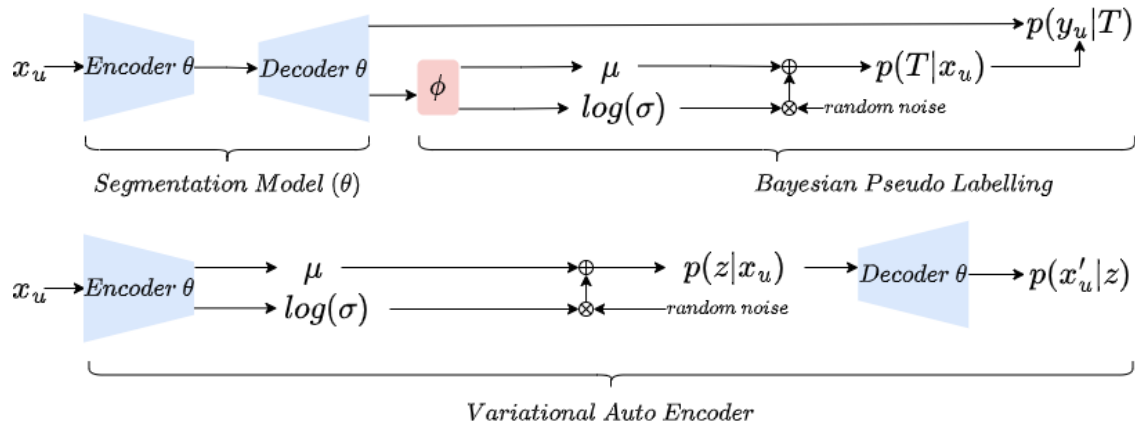


Figure 3: Comparison between BPL and VAE in details. For BPL, only unsupervised learning part is illustrated.

with differing numbers of labelled volumes at: 2, 5, 10, 20. Normalisation was performed at case wise. Data curation resulted in 479 volumes for testing, which is equivalent to 1437 images. No data augmentation is used.

**BRATS 2018** We use BRATS 2018 [43] for demonstration of 2D multi-class segmentation of brain tumour of MRI images. The BRATS 2018 comprises 210 high-grade glioma and 76 low-grade glioma MRI cases. Each case contains 155 slices. We focus on multi-class segmentation of sub-regions of tumours in high grade gliomas (HGG). All slices were centre-cropped to 176 x 176. We prepared three different sets of 2D slices for labelled training data: 50 slices from one case, 150 slices from one case and 300 slices from two cases. We use another 2 cases for unlabelled training data and 1 case for validation. 50 HGG cases were randomly sampled for testing. Case-wise normalisation was performed and all modalities were concatenated. A total of 3433 images were included for testing. No data augmentation is used.

**Task01 Brain Tumour** We use Task01 Brain Tumour from Medical Segmentation Decathlon consortium [44] as a demonstration of 3D binary segmentation of brain tumour of MRI images. The Task01 Brain Tumour is based on BRATS 2017 with different naming format from BRATS 2018. This data set was not in our previous MICCAI version but we included this data set here because it is easy to download and use for the readers for the future follow-up works. Each case in The Task01 Brain Tumour has 155 slices with 240 x 240 spatial dimension. We merge all of the tumour classes into one tumour class for simplicity. We do not apply centre cropping in the pre-processing here. In the training, we randomly crop volumes on the fly with size of 64 x 64 x 64. We separate the original training cases as labelled training data and testing data. We use the original testing cases as unlabelled data. For the labelled training data, we use 8 cases with index number from 1 to 8. We have 476 cases for testing and 266 cases for unlabelled training data. We apply normalisation with statistics of intensities across the whole training data set. We keep all of the MRI modalities as 4 channel input.

## 6.2 Baselines

Our baselines include both supervised and semi-supervised learning methods. We use U-net [45] in SegPL as an example of segmentation network. Partly due to computational constraints, for 3D experiments we used a 3D U-net with 8 channels in the first encoder such that unlabelled data can be included in the same batch. For 2D experiments, we used a 2D U-net with 16 channels in the first encoder. The first baseline utilises supervised training on the backbone and is trained with labelled data denoted as ‘‘Sup’’. We compared SegPL with state-of-the-art consistency based methods: 1) ‘‘cross pseudo supervision’’ or CPS [13], which is considered the current state-of-the-art for semi-supervised segmentation; 2) another recent state-of-the-art model ‘‘cross consistency training’’ [12], denoted as ‘‘CCT’’, due to hardware restriction, our implementation shares most of the decoders apart from the last convolutional block; 3) a classic model called ‘‘FixMatch’’ (FM) [5]. To adapt FixMatch for a segmentation task, we added Gaussian noise as weak augmentation and ‘‘RandomAug’’ [46] for strong augmentation; 4) ‘‘self-loop [47]’’, which solves a self-supervised jigsaw problem as pre-training and combines with pseudo-labelling.

Table 1: Hyper-parameters used across experiments. Different data might need different  $\alpha$ .

Data	Batch Size	Learning rate	Steps	$\alpha$	Unlabelled/labelled
BRATS(2D)	2	0.03	200	0.05	5
CARVE(3D)	2	0.01	800	1.0	4
Task01(3D)	1	0.0004	25000	0.1	2

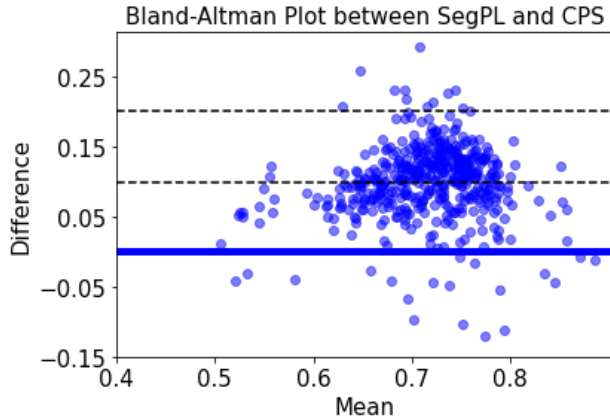


Figure 4: SegPL statistically outperforms the best performing baseline CPS when trained on 2 labelled volumes from the CARVE dataset. Each data point represents a single testing image.

### 6.3 Training

We use Adam optimiser[48] with default settings. Our code is implemented using Pytorch 1.0[38] and released in <https://github.com/moucheng2017/EMSSL>. We trained all of the experiments with a TITAN V GPU with 12GB memory. The training hyperparameters are included in Table 1.

### 6.4 Segmentation performances

The segmentation performances of CARVE 2014, BRATS 2018, Task 01 can be found in Tab.2, Tab.3 and Tab.4, respectively. As reflected in the quantitative results in tables, pseudo labelling based SegPL consistently achieves better results than the baselines of semi-supervised and supervised methods. Especially, as shown in Fig.4 of the Bland-Altman plot between the best performing baseline CPS and our SegPL on CARVE when only 2 labelled volumes are used for training, SegPL statistically outperforms the best baseline. We further confirm the statistical difference by performing Mann Whitney test on the same results on 2 labelled volumes and we found the p-value less than  $1e-4$ . By extending the SegPL with variational inference to SegPL-VI, we found further improvements on segmentation on most of the experiments. Interestingly, the improvements brought by SegPL-VI is more obvious on multi-class experiments on BRATS 2018. As the outputs on BRATS are multi-channel but SegPL-VI learns one threshold across all of the channel, we suspect that might bring in strong regularisation effect which results in noticeable improvements. We also noticed that SegPL-VI could fail to learn optimal threshold sometimes as the result of SegPL-VI on CARVE with 5 labelled volumes are inferior to the corresponding result of SegPL. We expect that more hyper-parameter searching could improve the performance of SegPL.

As shown in the qualitative results in Fig5 of CARVE, SegPL successfully learnt better decision boundary than other baselines that SegPL can partially separate the foreground lung vessels from the background whereas most of the other methods classifies everything as background. However, SegPL seemed to have overconfident predictions on the edges of the foreground that it has a lot of false positive results. Similarly in BRATS, SegPL detected one more class of brain tumour (blue) than the other baselines in Fig6. However, none of the methods including SegPL can detect the most rare green class of tumour.

One interesting result is shown in Tab.4 on 3D binary segmentation of whole tumour. During training, we use random cropping with fixed size at  $64 \times 64 \times 64$  to compensate with the memory of GPU. On testing data, we examined the models with different sizes of cropped volumes at  $32^3$ ,  $64^3$ ,  $96^3$  and  $128^3$ . The models actually generalise well on the scales that they haven't seen during the training. In fact, larger cropped volumes result in better results.

Table 2: Our model vs Baselines on a binary vessel segmentation task on 3D CT images of the CARVE dataset. Metric is Intersection over Union (IoU ( $\uparrow$ ) in %). Avg performance of 5 training. **blue: 2nd best. red: best**

Data	Supervised	Semi-Supervised				
Labelled Volumes	3D U-net [45](2015)	FixMatch [5](2020)	CCT [12](2020)	CPS [13](2021)	SegPL (Ours, 2022)	SegPL+VI (Ours, 2022)
2	56.79 $\pm$ 6.44	62.35 $\pm$ 7.87	51.71 $\pm$ 7.31	66.67 $\pm$ 8.16	<b>69.44<math>\pm</math>6.38</b>	<b>70.65<math>\pm</math>6.33</b>
5	58.28 $\pm$ 8.85	60.80 $\pm$ 5.74	55.32 $\pm$ 9.05	70.61 $\pm$ 7.09	<b>76.52<math>\pm</math>9.20</b>	<b>73.33<math>\pm</math>8.61</b>
10	67.93 $\pm$ 6.19	72.10 $\pm$ 8.45	66.94 $\pm$ 12.22	75.19 $\pm$ 7.72	<b>79.51<math>\pm</math>8.14</b>	<b>79.73<math>\pm</math>7.24</b>
20	81.40 $\pm$ 7.45	80.68 $\pm$ 7.36	80.58 $\pm$ 7.31	81.65 $\pm$ 7.51	<b>83.08<math>\pm</math>7.57</b>	<b>83.41<math>\pm</math>7.14</b>
Computational need						
Train(s)	1014	2674	4129	2730	1601	1715
Flops	6.22	12.44	8.3	12.44	6.22	6.23
Para(K)	626.74	626.74	646.74	1253.48	626.74	630.0

Table 3: Our model vs Baselines on multi-class tumour segmentation on 2D MRI images of BRATS 2018. Metric is Intersection over Union (IoU ( $\uparrow$ ) in %). Avg performance of 5 runs. **blue: 2nd best. red: best**

Data	Supervised	Semi-Supervised				
Labelled Slices	2D U-net [45](2015)	Self-Loop [47](2020)	FixMatch [5](2020)	CPS [13](2021)	SegPL (Ours, 2022)	SegPL+VI (Ours, 2022)
50	54.08 $\pm$ 10.65	65.91 $\pm$ 10.17	67.35 $\pm$ 9.68	63.89 $\pm$ 11.54	<b>70.60<math>\pm</math>12.57</b>	<b>71.20<math>\pm</math>12.77</b>
150	64.24 $\pm$ 8.31	68.45 $\pm$ 11.82	69.54 $\pm$ 12.89	69.69 $\pm$ 6.22	<b>71.35<math>\pm</math>9.38</b>	<b>72.93<math>\pm</math>12.97</b>
300	67.49 $\pm$ 11.40	70.80 $\pm$ 11.97	70.84 $\pm$ 9.37	71.24 $\pm$ 10.80	<b>72.60<math>\pm</math>10.78</b>	<b>75.12<math>\pm</math>13.31</b>

Table 4: Our model vs Supervised baseline on 3D binary tumour segmentation of Task 01 Brain Tumour (BRATS 2017). Metric is Intersection over Union (IoU ( $\uparrow$ ) in %). Avg performance of models between iteration 20000 and 25000 with 1000 as the interval. **red: best**

Testing size	32 <sup>3</sup>	64 <sup>3</sup>	96 <sup>3</sup>	128 <sup>3</sup>
Supervised	61.07 $\pm$ 7.93	66.94 $\pm$ 12.4	70.13 $\pm$ 13.22	72.09 $\pm$ 12.48
SegPL-VI	<b>64.44<math>\pm</math>8.3</b>	<b>71.43<math>\pm</math>11.91</b>	<b>73.07<math>\pm</math>11.71</b>	<b>74.48<math>\pm</math>11.51</b>

Although SegPL achieves higher segmentation accuracy, SegPL enjoys a low computational burden. As illustrated in the computational need section in Tab.2, SegPL has the least computational burden among all of the tested semi-supervised learning baselines. Especially in terms of FLOPs, SegPL is very close to supervised learning methods. This shows that our model has the scaling potential for large models and large data sets.

## 6.5 Ablation studies on hyper-parameters

We performed brief ablation studies on hyper-parameters on BRATS with 150 labelled slices. As shown in Fig.7, a) shows that SegPL is very sensitive to learning rate that it should be at least 0.01. We found that other baselines also needed large learning rate. Fig.7.b) shows the impact of warm-up schedule of  $\alpha$  from 0 to final  $\alpha$  value. x axis is the length of linear warming-up of  $\alpha$  in terms of whole steps. It appears that SegPL is not sensitive to warm-up schedule of  $\alpha$ . Fig.7.c) illustrates the effect of the ratio between unlabelled images to labelled images in each batch. The suitable range of unlabelled/labelled ratio is quite wide and between 1 to 10. Fig.7.d) shows that the pseudo supervision cannot be too strong. This confirms the suggestions from the original pseudo labelling paper that pseudo supervision should not dominate the training.

## 6.6 Ablation studies on the prior of Bayesian Pseudo Labels

Figure 11 and 10 show that higher prior might result in better performance.

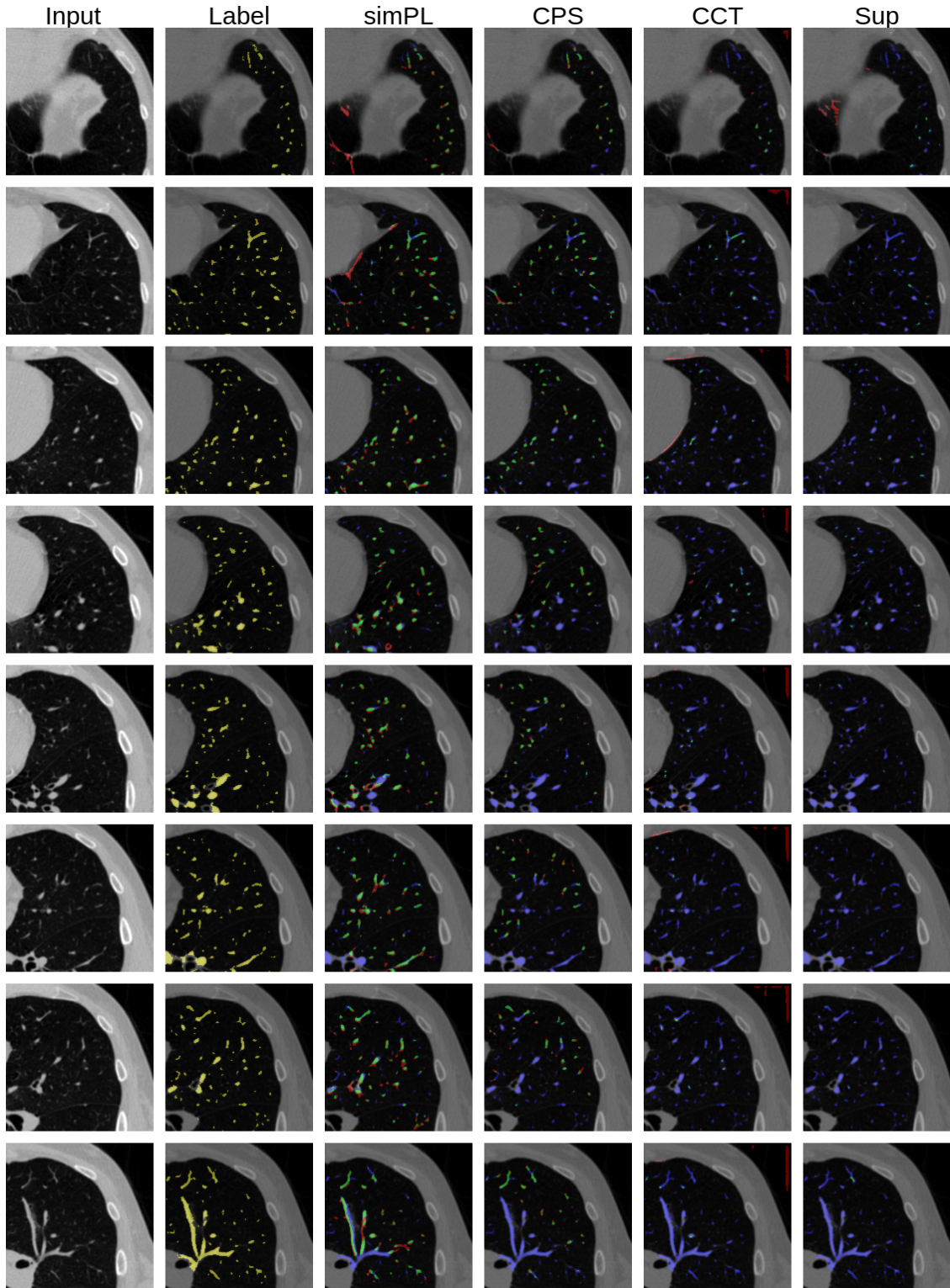


Figure 5: Visual results. CARVE trained with 5 labelled volumes. Red: false positive. Green: true positive. Blue: false negative. Yellow: ground truth. GT: Ground truth. CPS: cross pseudo labels (CVPR 2021). CCT: cross consistency training (CVPR 2020). Sup: supervised training.

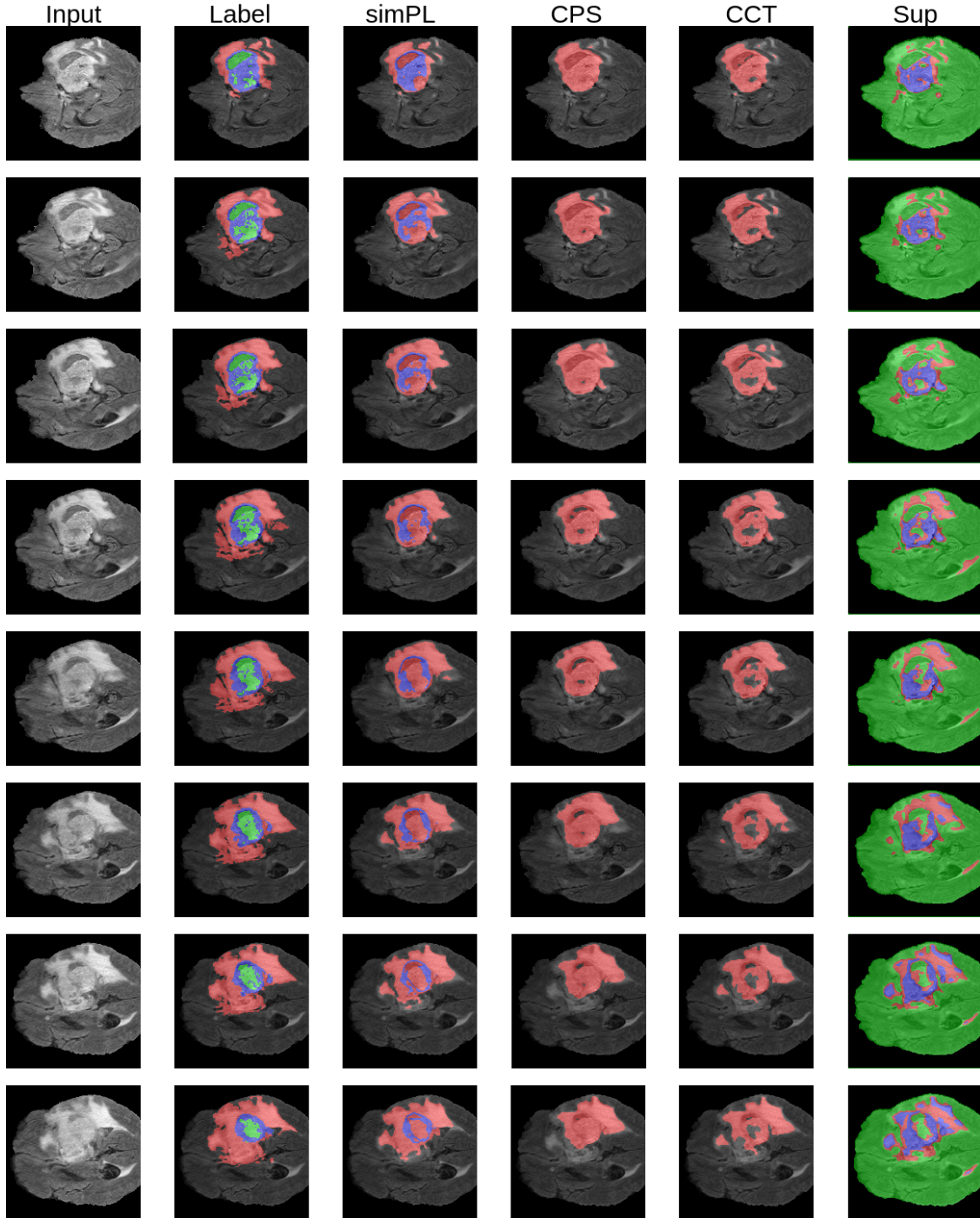


Figure 6: Visual results. BRATS 2018 trained with 300 labelled slices. Red: whole tumour. Green: tumour core. Blue: enhancing tumour core. GT: Ground truth. CPS: cross pseudo labels (CVPR 2021). CCT: cross consistency training (CVPR 2020). Sup: supervised training.

## 6.7 Robustness

Medical imaging normally suffer from out-of-the-distribution noises (e.g. variations in scan acquisition parameters and different patient populations) which significantly degenerate the trained model in real-life deployments. We investigate the robustness of SegPL on out-of-distribution (OOD) noise using models trained on CARVE. OOD noises are simulated

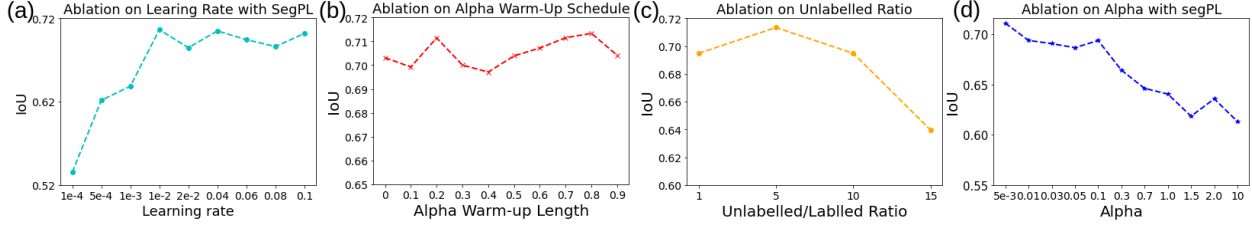


Figure 7: Ablation studies on BRATS with 150 labelled slices.

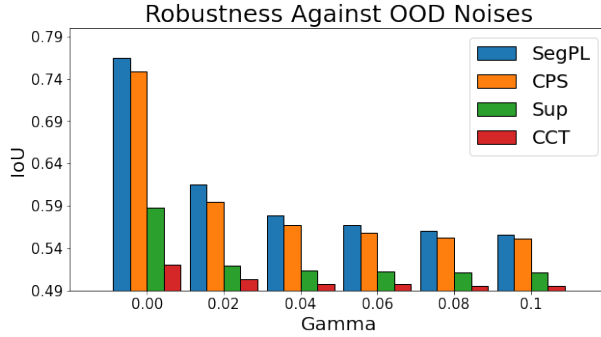


Figure 8: Robustness against out-of-distribution noise. Gamma is the strength of the out-of-distribution noises. Using 2 labelled volumes from CARVE.

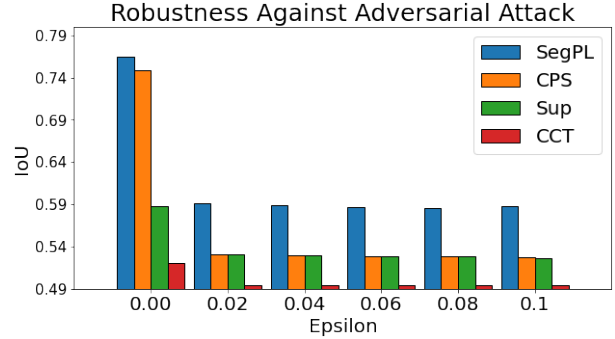


Figure 9: Robustness against adversarial attack. Epsilon is the strength of the FGSM[49] attack. Using 2 labelled volumes from CARVE.

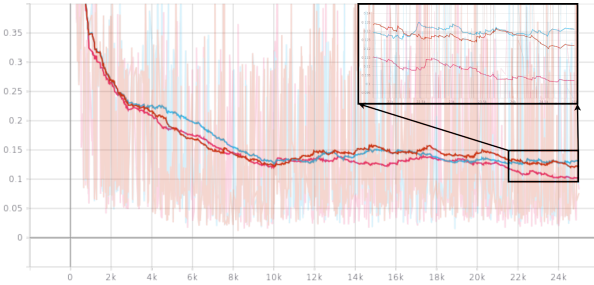


Figure 10: Ablation studies on priors of 0.4, 0.5 and 0.7. Y-axis: segmentation losses. X-axis: training iterations. Red: prior = 0.5. Blue: prior = 0.4. Pink: prior = 0.7. All trained on Task 01 Brain Tumour.



Figure 11: Ablation studies on priors of 0.4, 0.5 and 0.7. Y-axis: segmentation IoUs. X-axis: training iterations. Red: prior = 0.5. Blue: prior = 0.7. Dark blue: prior = 0.5. All trained on Task 01 Brain Tumour.

with unseen random contrast and Gaussian noise, we then apply mix-up [50] to create new testing samples by adding the OOD noises on original images. Specifically, for a given original testing image  $x_t$ , we applied random contrast and noise augmentation on  $x_t$  to derive OOD samples  $x'_t$ . We arrived at the testing sample ( $\hat{x}_t$ ) via  $\gamma x'_t + (1 - \gamma)x_t$ . As shown in Fig.8, as testing difficulty increases, the performances across all baselines drop exponentially. SegPL outperformed all of the baselines across all of the tested experimental settings. The findings suggest that SegPL is more robust when testing on OOD samples and achieves better generalisation performance against that from the baselines.

We also examined SegPL’s robustness against adversarial attack as privacy-preserving collaborative federated learning among hospitals has now become popular. We focus on using fast gradient sign method (FGSM)[49]. With increasing strength of adversarial attack (Epsilon), all the networks suffered performance drop. As shown in Fig.9, SegPL yet suffered much less than the baselines.

## 6.8 Uncertainty

Since SegPL-VI is trained with stochastic threshold for unlabelled data therefore not suffering from posterior collapse. Consequently, SegPL can generate plausible segmentation during inference using stochastic thresholds. To test the

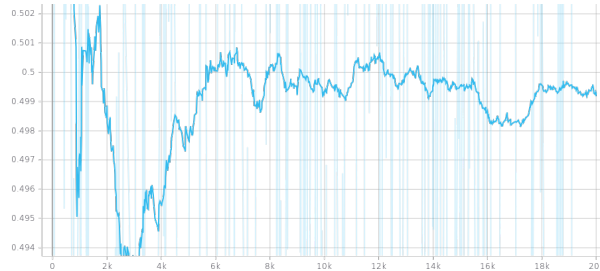


Figure 12: Learnt threshold with prior at 0.5 trained on Task 01 Brain Tumour.

performance of SegPL-VI on uncertainty quantification, we use random latent variable values (threshold) with 5 Monte Carlo samples. We focus experimenting on models trained with 5 labelled volumes of CARVE data set. For comparison, we adopt Deep Ensemble, as it is the gold-standard baseline for uncertainty estimation [51][52]. Both the tested methods Deep Ensemble and SegPL-VI achieved the same Brier score at 0.97. This result shows that SegPL-VI has the potential to become a benchmark method for uncertainty quantification. The Brier score is calculated using beneath equation, where,  $y_{ij}$  is the ground truth label at pixel at location  $i, j$ ,  $y_{ij}$  is 1 for foreground pixel and  $y_{ij}$  is 0 for background pixel.  $p_{ij}$  is the predicted probability of the pixel being the foreground pixel.

$$Brier = \frac{1}{HW} \sum_{i=1}^H \sum_{j=1}^W (p_{ij} - y_{ij})^2 \quad (21)$$

## 7 Limitations and future work

There are two main limitations of the proposed Bayesian pseudo labels. The first limitation is that once the model starts to over-fit, the model becomes overconfident that it predicts with very high confidence, while the learnt threshold also converges to oscillate around the prior mean (see an example of learnt threshold in Fig.12). In this situation, if the prior of the mean is too low, then the learnt threshold won't be able to mask out the bad over confident pseudo labels. Thus calibration becomes very important here. In future work, one could extend the formulation of pseudo labels to take into account of calibration. The second limitation is the use of the prior in the current paper. We use Gaussian due to its simplicity and easy to implement. However, Gaussian prior might not be the most optimal one here. Future work can explore the impact of other priors of learnt threshold. Candidate prior distributions include categorical and Beta distributions.

Another interesting future work can be studying the impact of labelled data in terms of preventing collapsed representations. Other futuer work can also look into the convergence property of SegPL-VI and improving SegPL-VI at uncertainty quantification. The feasibility of the applications of the proposed methods on other tasks such as classification and registration also remain unexplored.

## 8 Conclusions

In this paper, we interpret pseudo-labelling as EM and explore the potential improvement with variational inference following generalised EM. We hope this interperation can shed new lights on explainable AI. Empirically, we examined that the original pseudo-labelling [16] on semi-supervised medical image segmentation and we report that pseudo-labelling as a competitive and robust baseline. In the future pipeline for learning with limited annotations, we expect to exploits full potential if we combine semi-supervised learning with large-scale pre-training techniques.

## References

- [1] J. Kaplan, S. McCandlish, T. Henighan, T. Brown, B. Chess, R. Child, S. Gray, A. Radford, J. Wu, and D. Amodei, "Scaling laws for neural language models," <https://arxiv.org/pdf/2001.08361.pdf>, 2020.
- [2] X. Li, M. Jiang, X. Zhang, M. Kamp, and Q. Dou, "Fedbn: Federated learning on non-iid features via local batch normalization," *International Conference on Learning Representations (ICLR)*, 2021.
- [3] J. S. Bridle and D. J. M. Anthony Heading, "Unsupervised classifiers, mutual information and 'phantom targets'," *Advances in Neural Information Processing Systems (NeurIPS)*, 1991.

- [4] Y. Grandvalet and Y. Bengio, “Semi-supervised learning by entropy minimization,” *Neural Information Processing Systems (NeurIPS)*, 2004.
- [5] K. Sohn, D. Berthelot, C.-L. Li, Z. Zhang, N. Carlini, E. D. Cubuk, A. Kurakin, H. Zhang, and C. Raffel, “Fix-match: Simplifying semi-supervised learning with consistency and confidence,” *Neural Information Processing Systems (NeurIPS)*, 2020.
- [6] D. Berthelot, N. Carlini, E. D. Cubuk, A. Kurakin, H. Zhang, C. Raffel, and K. Sohn, “Remixmatch: Semi-supervised learning with distribution alignment and augmentation anchoring,” *International Conference On Learning Representation (ICLR)*, 2020.
- [7] X. Li, L. Yu, H. Chen, C. W. Fu, and P. A. Heng, “Semi-supervised skin lesion segmentation via transformation consistent self-ensembling model,” *British Machine Vision Conference (BMVC)*, 2018.
- [8] G. French, S. Laine, T. Aila, M. Mackiewicz, and G. aFinalyson, “Semi-supervised semantic segmentation needs strong, varied perturbations,” *British Machine Vision Conference (BMVC)*, 2020.
- [9] M.-C. Xu, Y.-K. Zhou, C. Jin, F. Wilson, S. Blumberg, M. de Groot, D. C. Alexander, N. P. Oxtoby, and J. Jacob, “Learning morphological feature perturbations for calibrated semi supervised segmentation,” *International Conference on Medical Imaging with Deep Learning (MIDL)*, 2022.
- [10] A. Tarvainen and H. Valpola, “Mean teachers are better role models: Weight-averaged consistency targets improve semi-supervised deep learning results,” *Neural Information Processing Systems (NeurIPS)*, 2017.
- [11] D. Berthelot, N. Carlini, I. Goodfellow, A. Oliver, N. Papernot, and C. Raffel, “Mixmatch: A holistic approach to semi-supervised learning,” *Neural Information Processing Systems (NeurIPS)*, 2019.
- [12] Y. Ouali, C. Hudelot, and M. Tami, “Semi-supervised semantic segmentation with cross-consistency training,” *Computer Vision and Pattern Recognition (CVPR)*, 2020.
- [13] X. Chen, Y. Yuan, G. Zeng, and J. Wang, “Semi-supervised semantic segmentation with cross pseudo supervision,” *Computer Vision and Pattern Recognition (CVPR)*, 2021.
- [14] M. N. Rizve, K. Duarte, Y. S. Rawat, and M. Shah, “In defense of pseudo-labelling: An uncertainty-aware pseudo-label selective framework for semi-supervised learning,” *International Conference on Learning Representation (ICLR)*, 2021.
- [15] M.-C. Xu, Y. Zhou, C. Jin, M. de Groot, D. C. Alexander, N. P. Oxtoby, Y. Hu, and J. Jacob, “Bayesian pseudo labels: Expectation maximization for robust and efficient semi-supervised segmentation,” *International Conference on Medical Image Computing and Computer Assisted Interventions (MICCAI)*, 2022.
- [16] D.-H. Lee, “Pseudo-label : The simple and efficient semi-supervised learning method for deep neural networks,” *ICML workshop on Challenges in Representation Learning*, 2013.
- [17] H. Pham, Z. Dai, Q. Xie, and Q. V. Le, “Meta pseudo labels,” *International Conference on Computer Vision (ICCV)*, 2021.
- [18] Y. Zou, Z. Zhang, H. Zhang, C.-L. Li, X. Bian, J.-B. Huang, and T. Pfister, “Pseudoseg: Designing pseudo labels for semantic segmentation,” *International Conference on Learning Representation (ICLR)*, 2021.
- [19] E. Arazo, D. Ortego, P. Albert, N. E. O’Connor, and K. McGuinness, “Pseudo-labeling and confirmation bias in deep semi-supervised learning,” <https://arxiv.org/abs/1908.02983>, 2019.
- [20] C. Chen, C. Qin, H. Qiu, C. Ouyang, S. Wang, L. Chen, G. Tarroni, W. Bai, and D. Rueckert, “Realistic adversarial data augmentation for mr image segmentation,” *International Conference on Medical Image Computing and Computer-Assisted Intervention (MICCAI)*, 2020.
- [21] K. Li, S. Wang, L. Yu, and P.-A. Heng, “Dual-teacher: Integrating intra-domain and inter-domain teachers for annotation-efficient cardiac segmentation,” *International Conference on Medical Image Computing and Computer-Assisted Intervention (MICCAI)*, 2020.
- [22] J. Xu, S. Lala, B. Gagoski, E. A. Turk, P. E. Grant, P. Golland, and E. Adalsteinsson, “Semi-supervised learning for fetal brain mri quality assessment with roi consistency,” *International Conference on Medical Image Computing and Computer-Assisted Intervention (MICCAI)*, 2020.
- [23] W. Hang, W. Feng, S. Liang, L. Yu, Q. Wang, K.-S. Choi, and J. Qin, “Local and global structure-aware entropy regularized mean teacher model for 3d left atrium segmentation,” *International conference on medical image computing and computer assisted intervention (MICCAI)*, 2020.
- [24] Y. Xie, J. Zhang, Z. Liao, J. Verjans, C. Shen, and Y. Xia, “Pairwise relation learning for semi-supervised gland segmentation,” *Medical Image Computing and Computer-Assisted Intervention (MICCAI)*, 2020.
- [25] K. Ta, S. S. Ahn, J. C. Stendahl, A. J. Sinusas, and J. S. Duncan, “A semi-supervised joint network for simultaneous left ventricular motion tracking and segmentation in 4d echocardiography,” *Medical Image Computing and Computer-Assisted Intervention (MICCAI)*, 2020.

- [26] M. N. N. To, S. Sankineni, S. Xu, B. Turkbey, P. A. Pinto, V. Moreno, M. Merino, B. J. Wood, and J. T. Kwak, "Improving dense pixelwise prediction of epithelial density using unsupervised data augmentation for consistency regularization," *Medical Image Computing and Computer-Assisted Intervention (MICCAI)*, 2020.
- [27] B. Unnikrishnan, C. M. Nguyen, S. Balaram, C. S. Foo, and P. Krishnaswamy, "Semi-supervised classification of diagnostic radiographs with noteacher: A teacher that is not mean," *Medical Image Computing and Computer-Assisted Intervention (MICCAI)*, 2020.
- [28] H. Yang, C. Shan, A. F. Kolen, and P. H. N. de With, "Deep q-network-driven catheter segmentation in 3d us by hybrid constrained semi-supervised learning and dual-unet," *Medical Image Computing and Computer-Assisted Intervention (MICCAI)*, 2020.
- [29] G. Fotedar, N. Tajbakhsh, S. Ananth, and X. Ding, "Extreme consistency: Overcoming annotation scarcity and domain shifts," *Medical Image Computing and Computer-Assisted Intervention (MICCAI)*, 2020.
- [30] L. Yu, S. Wang, X. Li, C.-W. Fu, and P.-A. Heng, "Uncertainty-aware self ensembling model for semi supervised 3d left atrium segmentation," *International Conference on Medical Image Computing and Computer Assisted Interventions (MICCAI)*, 2019.
- [31] X. Luo, M. Hu, T. Song, G. Wang, and S. Zhang, "Semi-supervised medical image segmentation via cross teaching between cnn and transformer," *International Conference on Medical Imaging with Deep Learning (MIDL)*, 2022.
- [32] W. Bai, O. Oktay, M. Sinclair, H. Suzuki, M. Rajchl, G. Tarroni, B. Glocker, A. King, P. M. Matthews, and D. Rueckert, "Semi-supervised learning for network-based cardiac mr image segmentation," *MICCAI*, 2017.
- [33] G. Wang, S. Zhai, G. Lasio, B. Zhang, B. Yi, S. Chen, T. J. Macvittie, D. Metaxas, J. Zhou, and S. Zhang, "Semi-supervised segmentation of radiationinduced pulmonary fibrosis from lung ct scans with multi-scale guided dense attention," *IEEE Transactions on Medical Imaging*, 2014.
- [34] Y. Wu, M. Xu, Z. Ge, J. Cai, and L. Zhang, "Semi-supervised left atrium segmentation with mutual consistency training," *MICCAI*, 2021.
- [35] J. Wang and T. Lukasiewicz, "Rethinking bayesian deep learning methods for semi-supervised volumetric medical image segmentation," *Computer Vision and Pattern Recognition (CVPR)*, 2022.
- [36] C. M. Bishop, *Pattern Recognition and Machine Learning (Information Science and Statistics)*. Berlin, Heidelberg: Springer-Verlag, 2006, ISBN: 0387310738.
- [37] O. Cahpelle, B. Scholkopf, and A. Zien, "Semi-supervised learning," *MIT Press*, 2006.
- [38] A. Paszke, S. Gross, F. Massa, A. Lerer, J. Bradbury, G. Chanan, T. Killeen, Z. Lin, N. Gimelshein, L. Antiga, A. Desmaison, A. Kopf, E. Yang, Z. DeVito, M. Raison, A. Tejani, S. Chilamkurthy, B. Steiner, L. Fang, J. Bai, and S. Chintala, "Pytorch: An imperative style, high-performance deep learning library," *Neural Information Processing System (NeurIPS)*, 2019.
- [39] F. Milletari, N. Navab, and S.-A. Ahmadi, "V-net: Fully convolutional neural networks for volumetric medical image segmentation," *International Conference on 3D Vision (3DV)*, 2016.
- [40] A. Dempster and D. R. N.M. Laird, "Maximum likelihood from incomplete data via the em algorithm," *Journal of the Royal Statistical Society. Series B (Methodological)*, 1977.
- [41] D. P. Kingma and M. Welling, "Auto-encoding variational bayes," *ICLR*, 2014.
- [42] J.-P. Charbonnier, M. Brink, F. Ciompi, E. T. Scholten, C. M. Schaefer-Prokop, and E. M. van Rikxoort, "Automatic pulmonary artery-vein separation and classification in computed tomography using tree partitioning and peripheral vessel matching," *IEEE Transaction on Medical Imaging*, 2015.
- [43] B. H. Menze, A. Jakab, S. Bauer, J. Kalpathy-Cramer, K. Farahani, J. Kirby, Y. Burren, N. Porz, J. Slotboom, and et al, "The multimodal brain tumor image segmentation benchmark (brats)," *IEEE Transaction on Medical Imaging*, 2015.
- [44] M. Antonelli, A. Reinke, S. Bakas, K. Farahani, A. Schneider, B. Landman, G. Ligjens, B. Menze, O. Ronneberger, R. Summers, B. Ginneken, M. Bilello, P. Bilic, P. Christ, R. Do, M. Gollub, S. H. Heckers, H. Huisman, W. R. Jarnagin, M. K. McHugo, S. Napel, J. S. G. Pernicka, K. Rhode, C. Tobon-Gomez, E. Vorontsov, J. A. Meakin, S. Ourselin, M. Wiesenfarth, P. Arbeláez, B. Bae, S. Chen, L. Daza, J. Feng, B. He, F. Isensee, Y. Ji, F. Jia, I. Kim, K. Maier-Hein, D. Merhof, A. Pai, B. Park, M. Perslev, R. Rezaiifar, O. Rippel, I. Sarasua, W. Shen, J. Son, C. Wachinger, L. Wang, Y. Wang, Y. Xia, D. Xu, Z. Xu, Y. Zheng, A. L. Simpson, L. Maier-Hein, and M. J. Cardoso, "The medical segmentation decathlon," *Nature Communications*, 2022.
- [45] O. Ronneberger, P. Fischer, and T. Brox, "U-net: Convolutional networks for biomedical image segmentations," *International conference on medical image computing and computer assisted intervention (MICCAI)*, 2015.
- [46] E. D. Cubuk, B. Zoph, J. Shlens, and Q. V. Le, "Randaugment: Practical automated data augmentation with a reduced search space," *Neural Information Processing Systems (NeurIPS)*, 2020.

- [47] Y. Li, J. Chen, X. Xie, K. Ma, and Y. Zheng, “Self-loop uncertainty: A novel pseudo-label for semi-supervised medical image segmentation,” *MICCAI*, 2020.
- [48] D. P. Kingma and J. Ba, “Adam: A method for stochastic optimization,” *International Conference on Learning Representation (ICLR)*, 2015.
- [49] A. Kurakin, I. J. Goodfellow, and S. Bengio, “Adversarial examples in the physical world,” *International Conference on Learning Representation Workshop*, 2017.
- [50] H. Zhang, M. Cisse, Y. N. Dauphin, and D. Lopez-Paz, “Mixup: Beyond empirical risk minimization,” *International Conference on Learning Representation (ICLR)*, 2018.
- [51] B. Lakshminarayanan, A. Pritzel, and C. Blundell, “Simple and scalable predictive uncertainty estimation using deep ensembles,” *Neural Information Processing System (NeurIPS)*, 2017.
- [52] Y. Ovadia, E. Fertig, J. Ren, Z. Nado, D. Sculley, S. Nowozin, J. V. Dillon, B. Lakshminarayanan, and J. Snoek, “Can you trust your model’s uncertainty? evaluating predictive uncertainty under dataset shift,” *Advances in Neural Information Processing Systems (NeurIPS)*, 2019.